

# Probing Magnetic and Vibrational Properties of Trigonal-Bipyramidal Co(II) and Ni(II) Complexes Using Advanced Spectroscopic Techniques

Michael J. Jenkins,<sup>a</sup> Mykhaylo Ozerov,<sup>b</sup> J. Krystek,<sup>b</sup> Luke L. Daemen,<sup>c</sup> Yongqiang Cheng,<sup>c</sup> Zi-Ling (Ben) Xue<sup>a,\*</sup>

<sup>a</sup> Department of Chemistry, University of Tennessee, Knoxville, Tennessee 37996, USA

<sup>b</sup> National High Magnetic Field Laboratory, Florida State University, Tallahassee, Florida 32310, USA

<sup>c</sup> Neutron Scattering Division, Oak Ridge National Laboratory, Oak Ridge, Tennessee 37831, USA

## Supporting Information

### Table of Contents

#### S1. Author contributions

#### S2. Co-MST-H<sub>2</sub>O. Additional results

- a. Powder X-ray diffraction of the **Co-MST-H<sub>2</sub>O** sample
- b. Additional FIRMS spectra
- c. Additional HFEPR spectra
- d. Additional INS spectra
- e. Powder neutron diffraction from VISION
- f. Symmetries and energies of calculated phonons
- g. Spin density
- h. Hirshfeld fingerprint plots

#### S3. Ni-MST-H<sub>2</sub>O. Additional results

- a. Powder X-ray diffraction of the **Ni-MST-H<sub>2</sub>O** sample
- b. FIRMS spectra
- c. Additional INS spectra
- d. Hirshfeld fingerprint plots

#### S4. Spin densities in [Co(12-crown-4)<sub>2</sub>](I<sub>3</sub>)<sub>2</sub> and Co(AsPh<sub>3</sub>)<sub>2</sub>I<sub>2</sub>

- a. [Co(12-crown-4)<sub>2</sub>](I<sub>3</sub>)<sub>2</sub>
- b. Co(AsPh<sub>3</sub>)<sub>2</sub>I<sub>2</sub>

## **S1. Author contributions**

- Michael J. Jenkins synthesized and characterized the complexes.
- Jenkins and M. Ozerov collected and interpreted FIRMS data.
- J. Krzystek performed HFEPR experiments, analyzed, and interpreted the results.
- L. L. Daemen and Y. Cheng collected INS at VISION. Jenkins processed and interpreted the results.
- Z. L. Xue initiated the project and supervised the research including data analysis and interpretation.
- Jenkins and Xue wrote the manuscript with input from all authors.

## S2. Co-MST-H<sub>2</sub>O. Additional results

### S2.a. Powder X-ray diffraction of the Co-MST-H<sub>2</sub>O samples

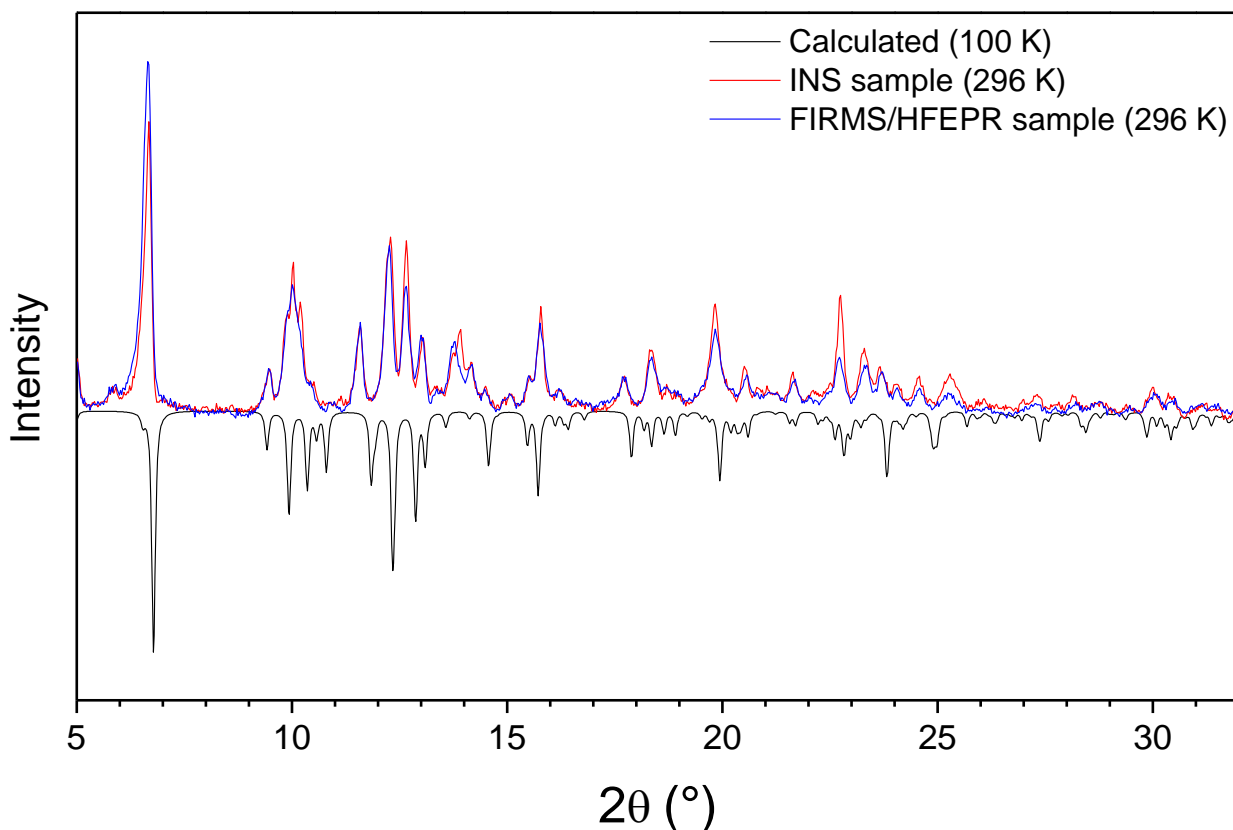


**Figure S1.** PXRD patterns at 296 K of **Co-MST-H<sub>2</sub>O** samples for INS and FIRMS/HFEPR compared to the calculated pattern from the reported single-crystal structure at 100 K.<sup>S1</sup>

There are no significant differences between the samples used for INS and FIRMS/HFEPR. The dehydration of **Co-MST-H<sub>2</sub>O** may be due to the experimental conditions used for the FIRMS experiment. In FIRMS, there is a significant low pressure ( $\sim 1.5 \times 10^{-4}$  mbar) while spectra are collected. There may have been cracks in the eicosane, leading to the exposure of the sample to low pressure and dehydration of **Co-MST-H<sub>2</sub>O** to **Co-MST**.

In INS, the **Co-MST-H<sub>2</sub>O** sample was sealed at ambient pressure in a metal sample can. Thus, dehydration is not likely.

**S2.b.** Additional FIRMS spectra

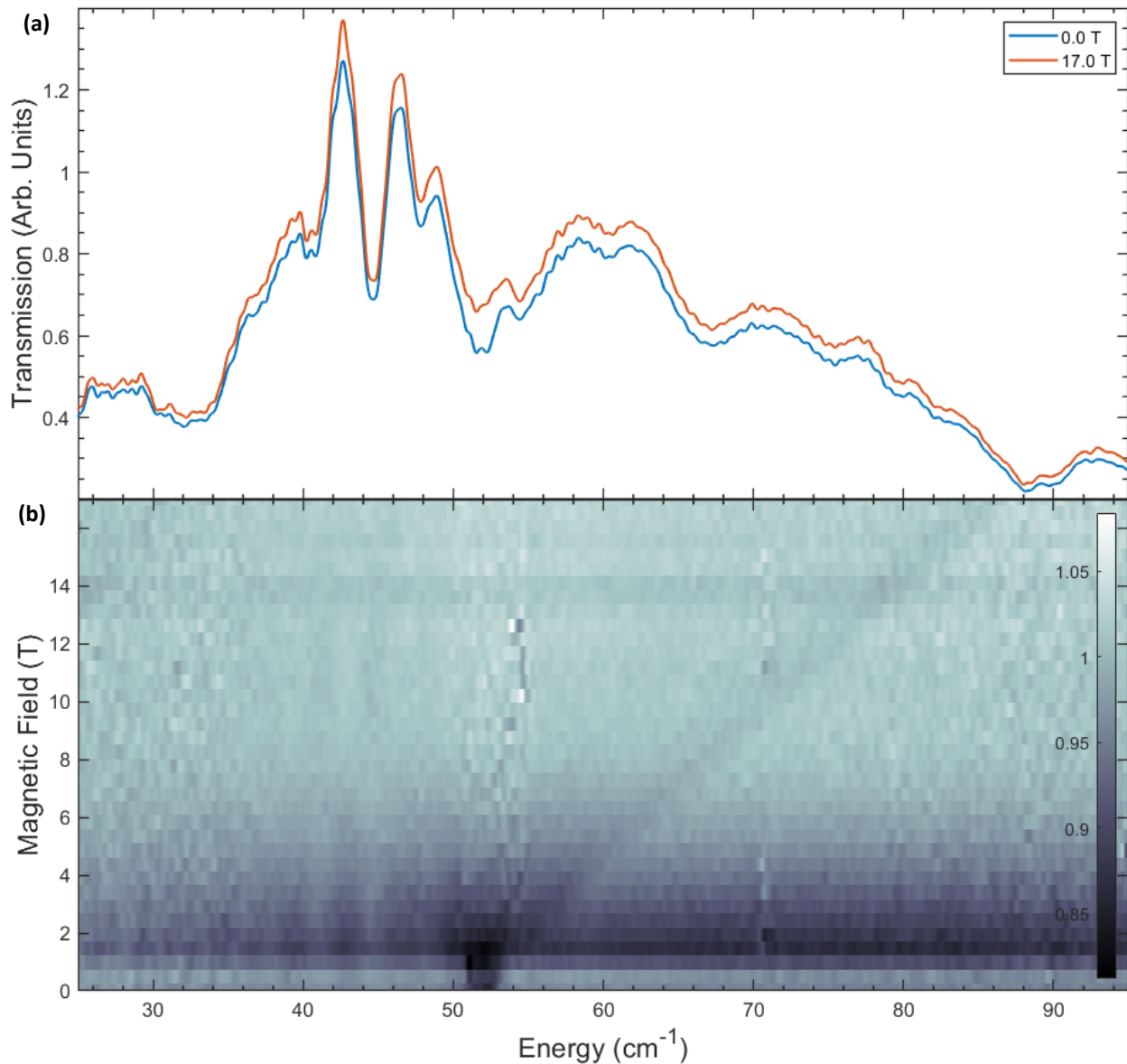


**Figure S2.** (a) FIRMS transmission spectra for a **Co-MST-H<sub>2</sub>O** sample placed in the Voigt configuration.<sup>S2</sup> (b) 2D plot of the normalized (by average) transmission. Figure 3 shows the FIRMS transmission spectra for a sample in the Faraday configuration.<sup>S2</sup> There is a greater field dependence of data collected by Voigt transmission.

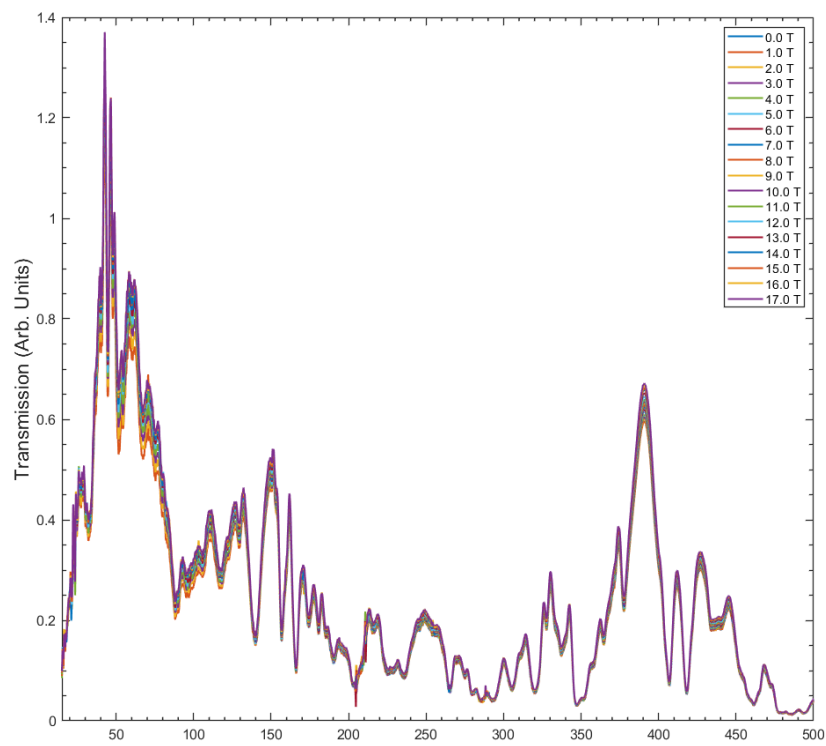


**Figure S3.** Averaged data of **Co-MST-H<sub>2</sub>O** with all T-value scans, showing phonon features at 10-500 cm<sup>-1</sup>.

**S2.c.** Additional HFEPR spectra

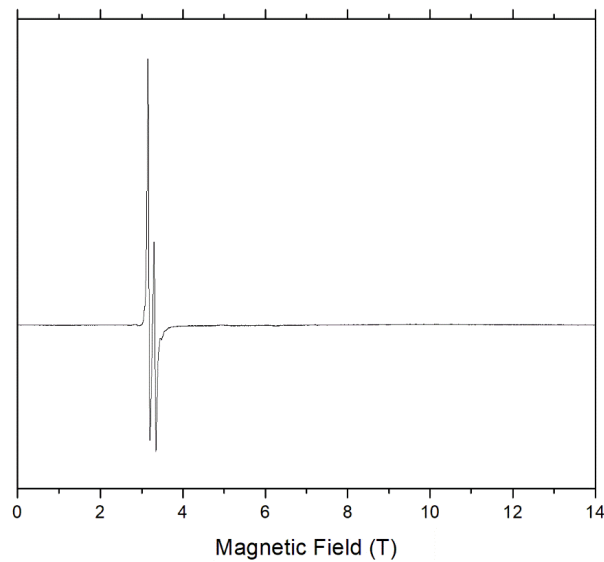


**Figure S4.** HFEPR spectrum of an unconstrained (loose) sample of **Co-MST-H<sub>2</sub>O** at 10 K and 203 GHz. The two resonances with different intensities correspond to different spin species A and B, with the lower intensity being that of B. Species A can be identified as compound **Co-MST-H<sub>2</sub>O**, and species B as the dehydrated compound **Co-MST**.

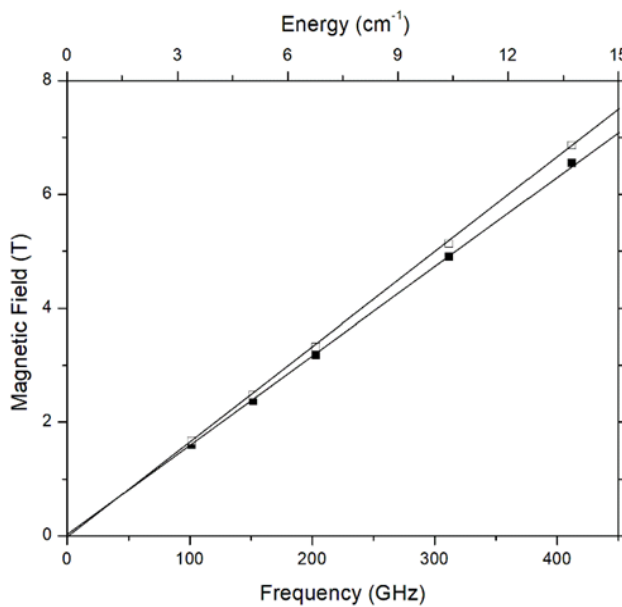


**Figure S5.** Frequency dependence of the EPR resonances observed in the unconstrained (loose) sample of **Co-MST-H<sub>2</sub>O** at 10 K and 203 GHz. The lines correspond to g-values of 2.20 and 2.30 for the high-intensity (A) and low-intensity (B) resonances respectively.

**S2.d.** Additional INS spectra

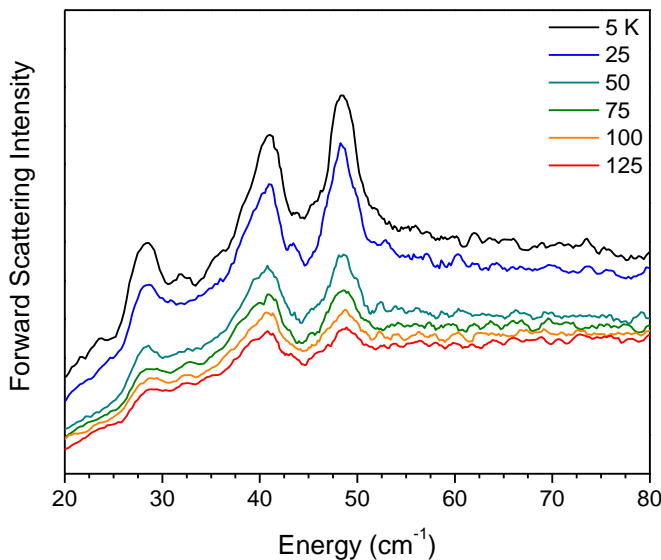


**Figure S6.** Forward scattering spectra of **Co-MST-H<sub>2</sub>O** at 20-80 cm<sup>-1</sup>. There are two temperature-dependent peaks at 28.5 and 40.2 cm<sup>-1</sup> that are not in the backward scattering spectra in Figure 5. These peaks show both temperature and Q dependence ( $\vec{Q} = \vec{k}_i - \vec{k}_f$  is the momentum transfer and Q is the magnitude of  $\vec{Q}$ , where  $k_i$  refers to the momentum of the incoming neutron and  $k_f$  of the outgoing neutron.).<sup>S3</sup> The observations suggest the peaks are magnetic. The sources giving these peaks are not clear. Impurities from degradation of **Co-MST-H<sub>2</sub>O** or starting materials may contribute to these peaks, though they were not observed in PXRD (Figure S1).

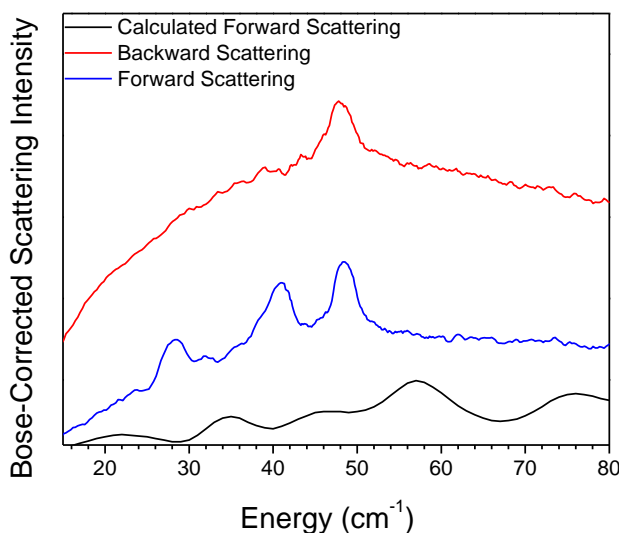


**Figure S7.** INS spectra of **Co-MST-H<sub>2</sub>O** at 5 K in comparison with the calculated phonon spectrum in the low energy (15-80 cm<sup>-1</sup>) region with both forward- and back-scattering spectra.

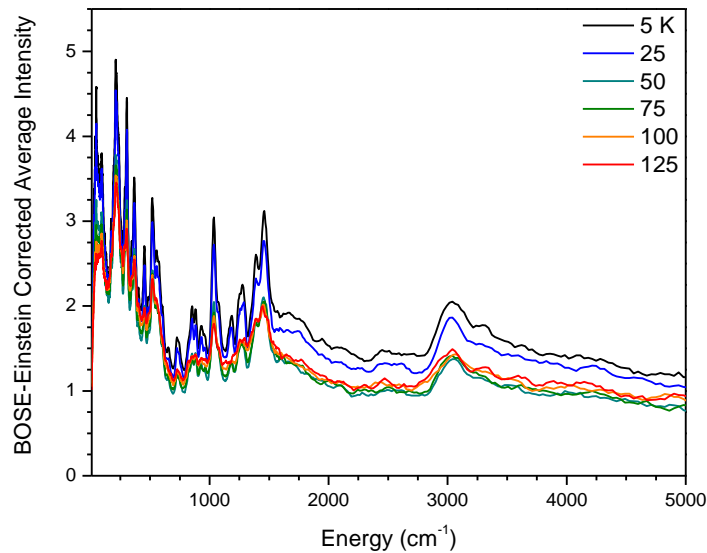


**Figure S8.** INS spectra of **Co-MST-H<sub>2</sub>O** at 10-5000 cm<sup>-1</sup>.

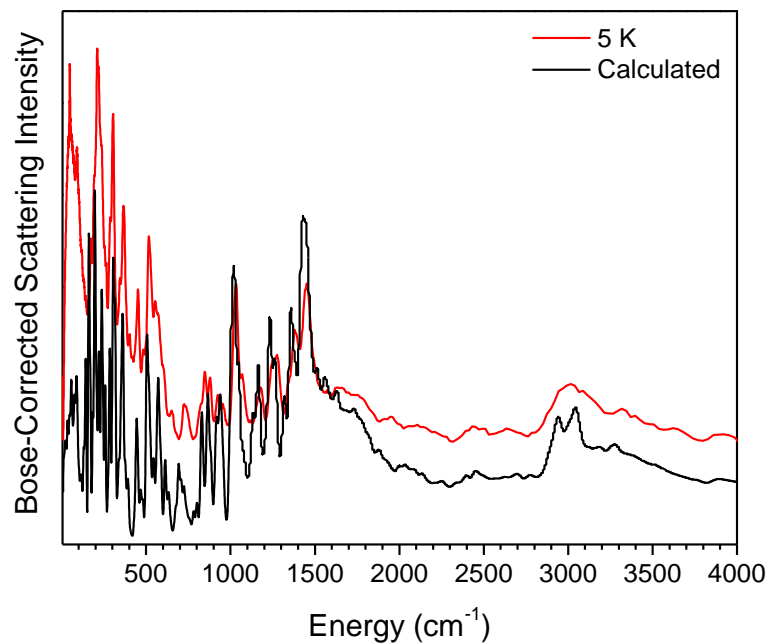


**Figure S9.** Calculated vs experimental spectra of **Co-MST-H<sub>2</sub>O** at 5-4000 cm<sup>-1</sup>. Differences between the calculated and 5 K spectra are not sufficient to determine magnetic excitations clearly.

**S2.e.** Powder neutron diffraction from VISION

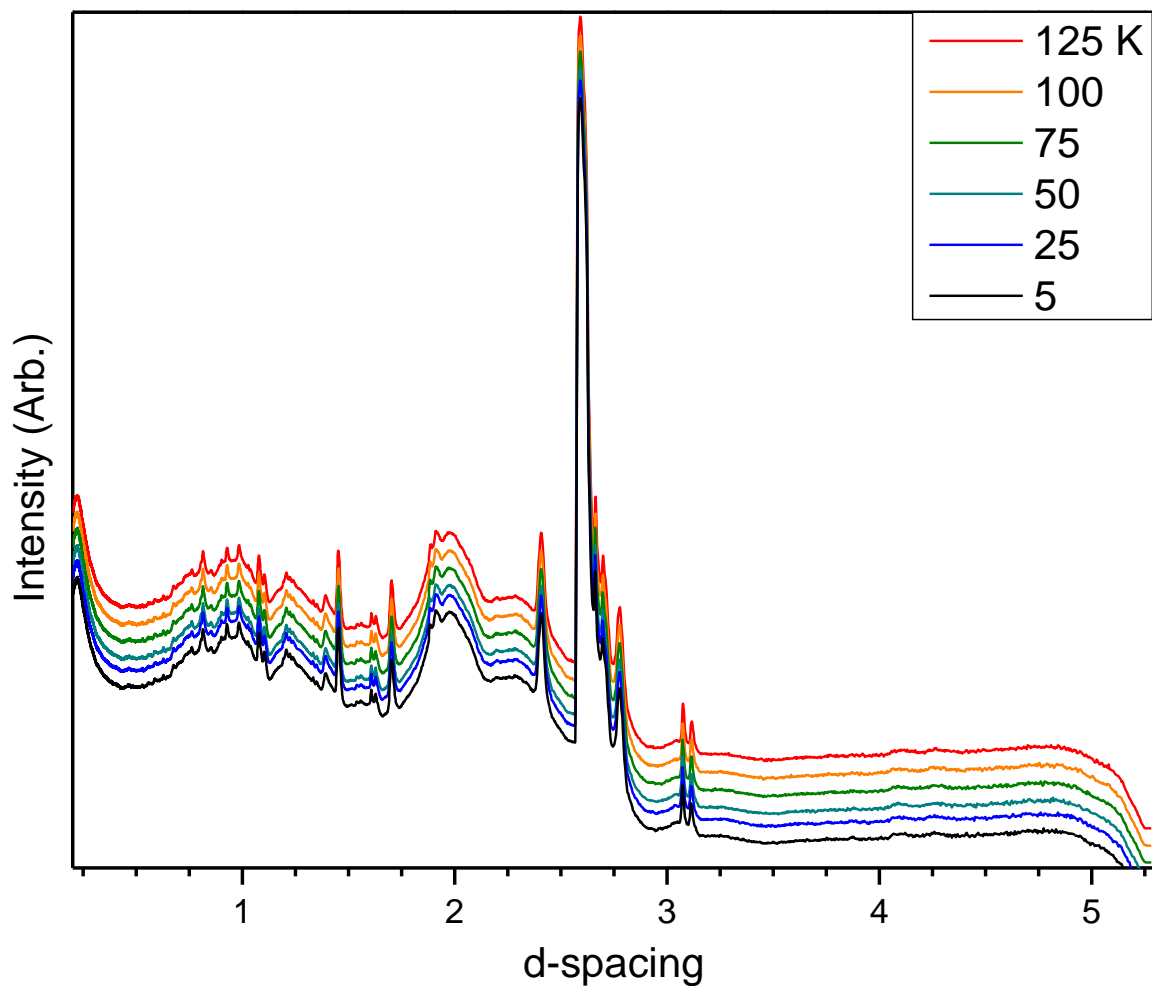


**Figure S10.** Waterfall powder neutron diffraction from VISION for **Co-MST-H<sub>2</sub>O**. Lack of changes to peak shape and location indicates a lack of phase change from high to low temperature.

**S2.f.** Calculated phonons

**Table S1.** Calculated phonons from VASP calculations for **Co-MST-H<sub>2</sub>O** with symmetry

Phonon No.	Frequency (cm <sup>-1</sup> )	Symmetry	Phonon No.	Frequency (cm <sup>-1</sup> )	Symmetry
1	5.28	$A_u$	34	68.05	$A_g$
2	6.54	$A_g$	35	68.71	$A_u$
3	13.57	$A_u$	36	70.51	$A_g$
4	18.02	$A_g$	37	70.54	$A_u$
5	19.61	$A_u$	38	73.93	$A_u$
6	25.18	$A_g$	39	75.65	$A_g$
7	27.86	$A_g$	40	76.73	$A_g$
8	28.58	$A_u$	41	77.25	$A_u$
9	29.88	$A_u$	42	80.22	$A_g$
10	30.21	$A_g$	43	80.95	$A_u$
11	32.51	$A_g$	44	83.72	$A_g$
12	35.06	$A_g$	45	84.85	$A_u$
13	35.27	$A_u$	46	85.95	$A_g$
14	37.90	$A_g$	47	87.16	$A_u$
15	37.94	$A_g$	48	89.18	$A_g$
16	38.69	$A_u$	49	90.55	$A_u$
17	42.08	$A_u$	50	92.02	$A_g$
18	44.37	$A_g$	51	92.40	$A_g$
19	45.11	$A_u$	52	93.08	$A_u$
20	45.69	$A_u$	53	96.56	$A_g$
21	45.98	$A_u$	54	96.63	$A_u$
22	46.76	$A_g$	55	100.42	$A_u$
23	47.65	$A_g$	56	101.22	$A_g$
24	50.62	$A_g$	57	102.21	$A_g$
25	53.95	$A_g$	58	107.21	$A_u$
26	54.59	$A_u$	59	107.65	$A_g$
27	56.59	$A_g$	60	109.69	$A_u$
28	56.95	$A_u$	61	115.81	$A_g$
29	58.28	$A_u$	62	116.33	$A_u$
30	60.62	$A_g$	63	117.90	$A_g$
31	60.83	$A_u$	64	122.31	$A_u$
32	65.85	$A_u$	65	122.64	$A_g$
33	66.44	$A_g$	66	127.63	$A_u$

67	130.80	$A_g$	103	211.43	$A_u$
68	131.07	$A_u$	104	211.68	$A_g$
69	133.40	$A_u$	105	216.35	$A_g$
70	135.09	$A_g$	106	216.95	$A_u$
71	138.77	$A_g$	107	218.45	$A_g$
72	139.50	$A_u$	108	218.86	$A_u$
73	145.17	$A_u$	109	220.10	$A_u$
74	145.86	$A_g$	110	220.61	$A_g$
75	156.06	$A_u$	111	222.35	$A_u$
76	156.78	$A_g$	112	223.88	$A_g$
77	159.28	$A_g$	113	224.99	$A_u$
78	159.95	$A_u$	114	227.96	$A_g$
79	162.57	$A_g$	115	233.18	$A_g$
80	164.09	$A_g$	116	233.76	$A_u$
81	164.25	$A_u$	117	235.68	$A_g$
82	166.05	$A_u$	118	236.14	$A_u$
83	168.56	$A_u$	119	237.87	$A_g$
84	169.94	$A_g$	120	239.85	$A_u$
85	171.87	$A_u$	121	240.53	$A_g$
86	172.98	$A_g$	122	240.95	$A_u$
87	182.18	$A_g$	123	245.00	$A_u$
88	182.81	$A_u$	124	247.39	$A_g$
89	186.80	$A_u$	125	256.11	$A_g$
90	187.24	$A_g$	126	257.90	$A_u$
91	193.20	$A_g$	127	259.59	$A_g$
92	193.39	$A_u$	128	260.55	$A_u$
93	193.70	$A_u$	129	271.80	$A_g$
94	195.54	$A_g$	130	272.32	$A_u$
95	197.95	$A_u$	131	275.44	$A_u$
96	198.63	$A_g$	132	275.93	$A_g$
97	199.05	$A_u$	133	277.26	$A_u$
98	205.10	$A_g$	134	278.57	$A_g$
99	205.44	$A_g$	135	281.31	$A_u$
100	205.86	$A_u$	136	281.62	$A_g$
101	207.26	$A_u$	137	284.11	$A_g$
102	208.16	$A_g$	138	286.56	$A_g$

139	287.01	$A_u$	175	363.30	$A_u$
140	288.11	$A_u$	176	363.85	$A_g$
141	297.50	$A_u$	177	365.84	$A_u$
142	298.59	$A_g$	178	366.43	$A_g$
143	298.99	$A_u$	179	376.66	$A_g$
144	300.43	$A_g$	180	376.96	$A_u$
145	303.76	$A_g$	181	387.47	$A_g$
146	303.96	$A_u$	182	387.57	$A_u$
147	304.45	$A_g$	183	394.11	$A_u$
148	307.06	$A_u$	184	394.60	$A_g$
149	307.42	$A_g$	185	432.00	$A_u$
150	308.13	$A_u$	186	432.07	$A_g$
151	310.30	$A_u$	187	441.70	$A_u$
152	311.24	$A_g$	188	442.84	$A_g$
153	315.05	$A_g$	189	444.14	$A_g$
154	317.06	$A_u$	190	445.79	$A_u$
155	317.10	$A_g$	191	451.01	$A_g$
156	318.03	$A_u$	192	453.18	$A_u$
157	331.81	$A_g$	193	467.02	$A_u$
158	332.52	$A_u$	194	467.44	$A_g$
159	338.58	$A_u$	195	471.72	$A_u$
160	340.71	$A_g$	196	472.43	$A_g$
161	341.06	$A_u$	197	480.83	$A_u$
162	341.78	$A_g$	198	481.37	$A_g$
163	347.96	$A_g$	199	498.82	$A_u$
164	348.97	$A_u$	200	500.01	$A_g$
165	351.53	$A_g$	201	504.35	$A_u$
166	352.32	$A_u$	202	504.86	$A_g$
167	353.65	$A_g$	203	505.13	$A_u$
168	354.22	$A_u$	204	505.14	$A_g$
169	358.84	$A_u$	205	505.63	$A_u$
170	359.02	$A_g$	206	506.94	$A_g$
171	360.09	$A_g$	207	508.01	$A_u$
172	360.71	$A_g$	208	508.39	$A_g$
173	360.78	$A_u$	209	512.95	$A_u$
174	360.98	$A_u$	210	513.48	$A_g$

211	515.49	$A_g$	247	585.91	$A_g$
212	515.97	$A_u$	248	586.80	$A_g$
213	517.29	$A_g$	249	589.28	$A_g$
214	517.30	$A_u$	250	591.27	$A_u$
215	518.51	$A_u$	251	612.89	$A_g$
216	518.58	$A_g$	252	613.21	$A_u$
217	520.23	$A_g$	253	621.57	$A_g$
218	520.30	$A_u$	254	621.66	$A_u$
219	522.45	$A_g$	255	628.93	$A_u$
220	524.07	$A_u$	256	629.88	$A_g$
221	527.38	$A_u$	257	634.94	$A_g$
222	527.82	$A_g$	258	635.69	$A_u$
223	528.82	$A_g$	259	675.29	$A_u$
224	529.49	$A_u$	260	676.83	$A_u$
225	538.39	$A_u$	261	676.99	$A_g$
226	538.77	$A_g$	262	681.78	$A_g$
227	544.75	$A_u$	263	691.93	$A_u$
228	545.03	$A_g$	264	693.76	$A_g$
229	545.05	$A_u$	265	706.29	$A_u$
230	545.62	$A_g$	266	706.52	$A_g$
231	549.94	$A_g$	267	707.97	$A_u$
232	550.71	$A_u$	268	709.09	$A_g$
233	559.47	$A_u$	269	711.29	$A_g$
234	560.77	$A_g$	270	711.31	$A_u$
235	565.91	$A_g$	271	723.49	$A_g$
236	566.10	$A_u$	272	723.71	$A_u$
237	567.55	$A_g$	273	737.90	$A_u$
238	567.94	$A_u$	274	738.29	$A_g$
239	568.70	$A_g$	275	781.20	$A_u$
240	570.92	$A_u$	276	782.05	$A_g$
241	572.15	$A_u$	277	800.10	$A_u$
242	573.25	$A_g$	278	800.47	$A_g$
243	574.66	$A_u$	279	824.72	$A_u$
244	576.79	$A_g$	280	825.25	$A_g$
245	584.39	$A_u$	281	828.33	$A_u$
246	585.89	$A_u$	282	830.43	$A_g$

283	833.11	$A_u$	319	947.48	$A_g$
284	836.82	$A_g$	320	947.97	$A_u$
285	843.75	$A_g$	321	952.14	$A_u$
286	843.87	$A_u$	322	952.28	$A_g$
287	855.87	$A_u$	323	955.68	$A_u$
288	860.35	$A_g$	324	956.07	$A_g$
289	865.80	$A_g$	325	958.85	$A_g$
290	865.82	$A_u$	326	959.04	$A_u$
291	867.80	$A_u$	327	994.19	$A_g$
292	869.53	$A_g$	328	994.23	$A_u$
293	869.83	$A_g$	329	996.29	$A_u$
294	870.01	$A_u$	330	996.39	$A_g$
295	883.57	$A_u$	331	997.67	$A_u$
296	885.66	$A_g$	332	997.69	$A_g$
297	908.69	$A_g$	333	1001.29	$A_g$
298	909.17	$A_u$	334	1001.87	$A_u$
299	914.40	$A_u$	335	1002.09	$A_g$
300	914.72	$A_g$	336	1002.71	$A_u$
301	917.87	$A_g$	337	1004.07	$A_g$
302	917.89	$A_u$	338	1004.68	$A_u$
303	918.29	$A_g$	339	1007.86	$A_g$
304	919.02	$A_u$	340	1008.07	$A_u$
305	919.68	$A_g$	341	1009.73	$A_u$
306	920.23	$A_u$	342	1009.76	$A_g$
307	920.63	$A_g$	343	1010.84	$A_u$
308	921.96	$A_u$	344	1011.63	$A_g$
309	930.93	$A_g$	345	1012.70	$A_u$
310	931.10	$A_u$	346	1013.24	$A_g$
311	932.48	$A_u$	347	1013.32	$A_u$
312	933.03	$A_g$	348	1014.23	$A_g$
313	935.14	$A_g$	349	1015.55	$A_u$
314	935.51	$A_u$	350	1015.97	$A_u$
315	939.29	$A_g$	351	1016.13	$A_g$
316	939.94	$A_u$	352	1016.44	$A_g$
317	941.63	$A_u$	353	1017.24	$A_g$
318	942.12	$A_g$	354	1017.31	$A_u$

355	1019.27	$A_g$	391	1073.87	$A_u$
356	1019.52	$A_u$	392	1075.46	$A_g$
357	1020.52	$A_g$	393	1077.94	$A_u$
358	1020.80	$A_u$	394	1082.16	$A_g$
359	1022.17	$A_u$	395	1127.84	$A_u$
360	1022.30	$A_g$	396	1128.88	$A_g$
361	1023.42	$A_g$	397	1132.39	$A_u$
362	1023.71	$A_u$	398	1133.54	$A_g$
363	1024.17	$A_u$	399	1134.71	$A_u$
364	1024.32	$A_g$	400	1134.98	$A_g$
365	1026.07	$A_u$	401	1145.51	$A_u$
366	1026.43	$A_g$	402	1146.13	$A_g$
367	1027.05	$A_u$	403	1150.09	$A_g$
368	1027.06	$A_g$	404	1152.89	$A_u$
369	1028.26	$A_g$	405	1154.28	$A_g$
370	1028.94	$A_u$	406	1154.33	$A_u$
371	1031.26	$A_u$	407	1161.55	$A_u$
372	1031.75	$A_u$	408	1162.93	$A_g$
373	1033.70	$A_u$	409	1165.87	$A_u$
374	1034.11	$A_g$	410	1165.92	$A_g$
375	1041.91	$A_g$	411	1167.04	$A_u$
376	1044.88	$A_u$	412	1167.11	$A_g$
377	1046.44	$A_g$	413	1169.61	$A_g$
378	1047.43	$A_u$	414	1169.66	$A_u$
379	1048.88	$A_g$	415	1183.92	$A_u$
380	1048.91	$A_u$	416	1187.04	$A_g$
381	1049.91	$A_g$	417	1212.63	$A_g$
382	1050.07	$A_u$	418	1213.84	$A_u$
383	1050.83	$A_u$	419	1226.74	$A_g$
384	1051.01	$A_g$	420	1228.11	$A_u$
385	1051.93	$A_u$	421	1230.27	$A_g$
386	1052.69	$A_g$	422	1230.45	$A_u$
387	1059.61	$A_u$	423	1230.49	$A_g$
388	1059.91	$A_g$	424	1230.74	$A_u$
389	1063.15	$A_u$	425	1234.53	$A_u$
390	1067.97	$A_g$	426	1234.55	$A_g$

427	1236.93	$A_u$	463	1350.40	$A_u$
428	1236.99	$A_g$	464	1350.57	$A_g$
429	1242.99	$A_g$	465	1351.99	$A_g$
430	1244.58	$A_u$	466	1352.21	$A_u$
431	1254.53	$A_g$	467	1353.00	$A_u$
432	1256.19	$A_u$	468	1353.35	$A_g$
433	1257.80	$A_g$	469	1354.91	$A_g$
434	1258.74	$A_u$	470	1355.40	$A_u$
435	1261.19	$A_u$	471	1356.22	$A_u$
436	1261.23	$A_g$	472	1356.23	$A_g$
437	1263.63	$A_g$	473	1359.59	$A_g$
438	1265.09	$A_u$	474	1360.00	$A_u$
439	1268.05	$A_g$	475	1360.81	$A_g$
440	1268.44	$A_u$	476	1360.86	$A_u$
441	1268.74	$A_g$	477	1362.41	$A_u$
442	1271.25	$A_u$	478	1362.52	$A_g$
443	1276.65	$A_g$	479	1367.25	$A_g$
444	1276.66	$A_u$	480	1367.27	$A_u$
445	1277.63	$A_u$	481	1369.21	$A_g$
446	1277.86	$A_g$	482	1370.20	$A_u$
447	1278.85	$A_g$	483	1371.06	$A_g$
448	1278.88	$A_u$	484	1371.66	$A_u$
449	1304.56	$A_u$	485	1381.23	$A_u$
450	1304.63	$A_g$	486	1381.34	$A_g$
451	1306.40	$A_g$	487	1382.45	$A_g$
452	1306.61	$A_u$	488	1382.78	$A_u$
453	1307.25	$A_g$	489	1382.89	$A_g$
454	1307.26	$A_u$	490	1383.28	$A_u$
455	1314.41	$A_g$	491	1385.25	$A_g$
456	1314.99	$A_u$	492	1385.55	$A_u$
457	1317.87	$A_g$	493	1386.11	$A_u$
458	1318.21	$A_u$	494	1386.77	$A_g$
459	1322.14	$A_g$	495	1387.41	$A_g$
460	1324.19	$A_u$	496	1388.21	$A_u$
461	1347.16	$A_g$	497	1388.31	$A_g$
462	1347.30	$A_u$	498	1389.47	$A_u$

499	1392.82	$A_g$	535	1431.86	$A_u$
500	1395.25	$A_u$	536	1433.13	$A_g$
501	1404.45	$A_u$	537	1434.90	$A_g$
502	1405.31	$A_g$	538	1434.91	$A_u$
503	1408.53	$A_u$	539	1436.51	$A_g$
504	1408.71	$A_g$	540	1436.92	$A_u$
505	1411.99	$A_g$	541	1439.95	$A_u$
506	1412.10	$A_u$	542	1440.18	$A_g$
507	1412.39	$A_g$	543	1440.32	$A_g$
508	1412.73	$A_g$	544	1441.80	$A_u$
509	1412.83	$A_u$	545	1442.79	$A_u$
510	1413.33	$A_u$	546	1443.39	$A_g$
511	1415.74	$A_u$	547	1444.37	$A_u$
512	1415.80	$A_g$	548	1444.53	$A_g$
513	1418.14	$A_g$	549	1445.42	$A_u$
514	1418.50	$A_u$	550	1445.83	$A_g$
515	1419.37	$A_g$	551	1446.66	$A_g$
516	1419.61	$A_u$	552	1447.13	$A_u$
517	1420.25	$A_g$	553	1448.11	$A_g$
518	1420.93	$A_u$	554	1449.92	$A_u$
519	1421.53	$A_g$	555	1451.65	$A_g$
520	1421.75	$A_u$	556	1451.67	$A_u$
521	1422.20	$A_u$	557	1452.60	$A_u$
522	1422.78	$A_g$	558	1452.70	$A_g$
523	1424.29	$A_g$	559	1455.60	$A_u$
524	1424.30	$A_u$	560	1455.78	$A_g$
525	1425.30	$A_u$	561	1456.63	$A_u$
526	1425.53	$A_g$	562	1457.70	$A_g$
527	1425.82	$A_g$	563	1459.48	$A_u$
528	1426.67	$A_u$	564	1460.09	$A_g$
529	1428.38	$A_u$	565	1466.93	$A_u$
530	1428.96	$A_g$	566	1471.04	$A_u$
531	1429.67	$A_u$	567	1471.08	$A_g$
532	1430.40	$A_u$	568	1477.37	$A_g$
533	1430.48	$A_g$	569	1477.46	$A_u$
534	1430.61	$A_g$	570	1482.57	$A_g$

571	1546.53	$A_g$	607	2935.92	$A_g$
572	1546.94	$A_u$	608	2935.92	$A_u$
573	1548.60	$A_u$	609	2936.20	$A_u$
574	1548.72	$A_g$	610	2936.71	$A_g$
575	1550.27	$A_u$	611	2938.22	$A_u$
576	1550.31	$A_g$	612	2938.29	$A_g$
577	1558.35	$A_g$	613	2938.50	$A_g$
578	1558.46	$A_u$	614	2938.61	$A_u$
579	1579.58	$A_g$	615	2939.34	$A_g$
580	1579.85	$A_u$	616	2939.47	$A_u$
581	1580.53	$A_g$	617	2941.53	$A_g$
582	1580.90	$A_u$	618	2941.58	$A_u$
583	1582.50	$A_g$	619	2942.41	$A_g$
584	1582.72	$A_u$	620	2942.45	$A_u$
585	1632.72	$A_u$	621	2946.28	$A_g$
586	1633.23	$A_g$	622	2946.54	$A_u$
587	2879.21	$A_u$	623	2950.72	$A_g$
588	2879.48	$A_g$	624	2950.83	$A_u$
589	2885.38	$A_u$	625	2950.99	$A_u$
590	2885.70	$A_g$	626	2951.35	$A_g$
591	2901.20	$A_u$	627	2953.75	$A_u$
592	2901.24	$A_g$	628	2954.10	$A_g$
593	2908.11	$A_u$	629	2961.56	$A_u$
594	2908.22	$A_g$	630	2962.23	$A_g$
595	2909.57	$A_g$	631	2964.35	$A_g$
596	2909.69	$A_u$	632	2964.48	$A_u$
597	2915.07	$A_u$	633	2966.21	$A_u$
598	2916.27	$A_g$	634	2967.51	$A_g$
599	2918.13	$A_u$	635	2971.85	$A_u$
600	2918.80	$A_g$	636	2972.66	$A_g$
601	2924.83	$A_u$	637	2983.05	$A_g$
602	2924.84	$A_g$	638	2983.13	$A_u$
603	2932.01	$A_g$	639	2983.98	$A_u$
604	2932.19	$A_u$	640	2984.00	$A_g$
605	2932.99	$A_g$	641	2988.48	$A_u$
606	2933.08	$A_u$	642	2988.48	$A_g$

643	2989.41	$A_g$	678	3040.86	$A_g$
644	2989.64	$A_u$	679	3041.14	$A_u$
645	2990.81	$A_g$	680	3041.77	$A_g$
646	2990.83	$A_u$	681	3041.95	$A_u$
647	2992.37	$A_u$	682	3042.46	$A_g$
648	2992.45	$A_g$	683	3043.68	$A_g$
649	2999.30	$A_g$	684	3043.72	$A_u$
650	2999.37	$A_u$	685	3046.92	$A_g$
651	2999.84	$A_g$	686	3047.07	$A_u$
652	3000.06	$A_u$	687	3047.58	$A_u$
653	3001.02	$A_g$	688	3047.95	$A_g$
654	3001.48	$A_u$	689	3048.28	$A_g$
655	3005.97	$A_g$	690	3048.29	$A_u$
656	3006.03	$A_u$	691	3049.57	$A_g$
657	3008.22	$A_u$	692	3049.64	$A_u$
658	3008.22	$A_g$	693	3052.67	$A_u$
659	3008.59	$A_g$	694	3053.37	$A_g$
660	3008.72	$A_u$	695	3054.18	$A_u$
661	3010.48	$A_u$	696	3055.10	$A_g$
662	3010.62	$A_g$	697	3056.64	$A_u$
663	3011.25	$A_u$	698	3056.66	$A_g$
664	3011.65	$A_g$	699	3070.15	$A_g$
665	3015.61	$A_g$	700	3070.26	$A_u$
666	3015.63	$A_u$	701	3073.66	$A_g$
667	3020.47	$A_g$	702	3076.40	$A_u$
668	3020.56	$A_u$	703	3104.96	$A_u$
669	3023.15	$A_g$	704	3105.52	$A_g$
670	3023.22	$A_u$	705	3183.24	$A_u$
671	3035.01	$A_g$	706	3184.84	$A_g$
672	3035.05	$A_u$	707	3283.62	$A_g$
673	3038.75	$A_g$	708	3283.72	$A_u$
674	3038.83	$A_u$	709	3401.30	$A_g$
675	3039.13	$A_u$	710	3403.19	$A_u$
676	3039.78	$A_g$	711	3526.00	$A_u$
677	3040.79	$A_u$	712	3526.95	$A_g$

## S2.g. Spin density

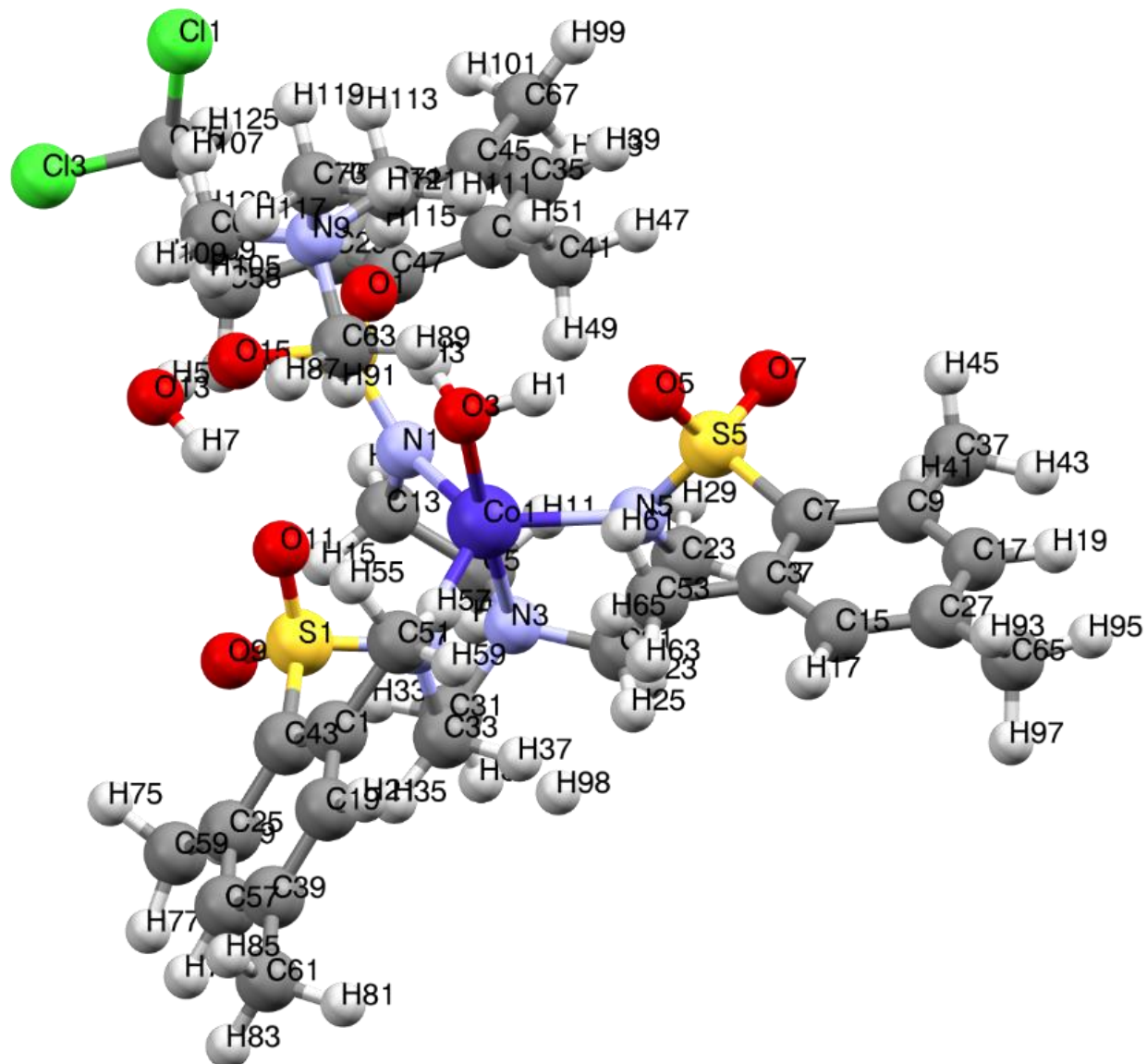


**Figure S11.** Structure of Co-MST-H<sub>2</sub>O with labels associated with spin density calculations.

**Table S2.** Spin densities of atoms from VASP calculations for **Co-MST-H<sub>2</sub>O**. There is a second identical molecule in the lattice and its spin density is not listed.

Atom label	Spin density	Atom label	Spin density	Atom label	Spin density
H1	0	H81	0	C35	0
H3	0	H83	0	C37	0
H5	0	H85	0	C39	0.001
H7	0	H87	0	C41	0
H9	0.001	H89	0	C43	0.002
H11	0	H91	0	C45	0.001
H13	0.001	H93	0	C47	0.002
H15	0.001	H95	0	C49	0
H17	0	H97	0	C51	0
H19	0	H99	0	C53	0
H21	0	H101	0	C55	0
H23	0.001	H103	0	C57	0
H25	0	H105	0	C59	0
H27	0.001	H107	0	C61	0
H29	0.001	H109	0	C63	0
H31	0.001	H111	0	C65	0
H33	0	H113	0	C67	0
H35	0.001	H115	0	C69	0
H37	0	H117	0	C71	0
H39	0	H119	0	C73	0
H41	0	H121	0	C75	0
H43	0	H123	0	N1	0.037
H45	0	H125	0	N3	0.045
H47	0	C1	0.001	N5	0.036
H49	0	C3	0.001	N7	0.037
H51	0	C5	0	N9	0
H53	0	C7	0.002	O1	0
H55	0	C9	0.001	O3	0.03
H57	0	C11	0.001	O5	0
H59	0	C13	-0.001	O7	0.006
H61	0	C15	0	O9	0.004
H63	0	C17	0	O11	0.001
H65	0	C19	0	O13	0

H67	0	C21	-0.001	O15	0.006
H69	0	C23	-0.001	S1	0.004
H71	0	C25	0.002	S3	0.005
H73	0	C27	0.001	S5	0.004
H75	0	C29	0.001	Cl1	0
H77	0	C31	0	Cl3	0
H79	0	C33	-0.001	Co1	2.627

**S2.h. Hirshfeld Surface Fingerprint Plots**

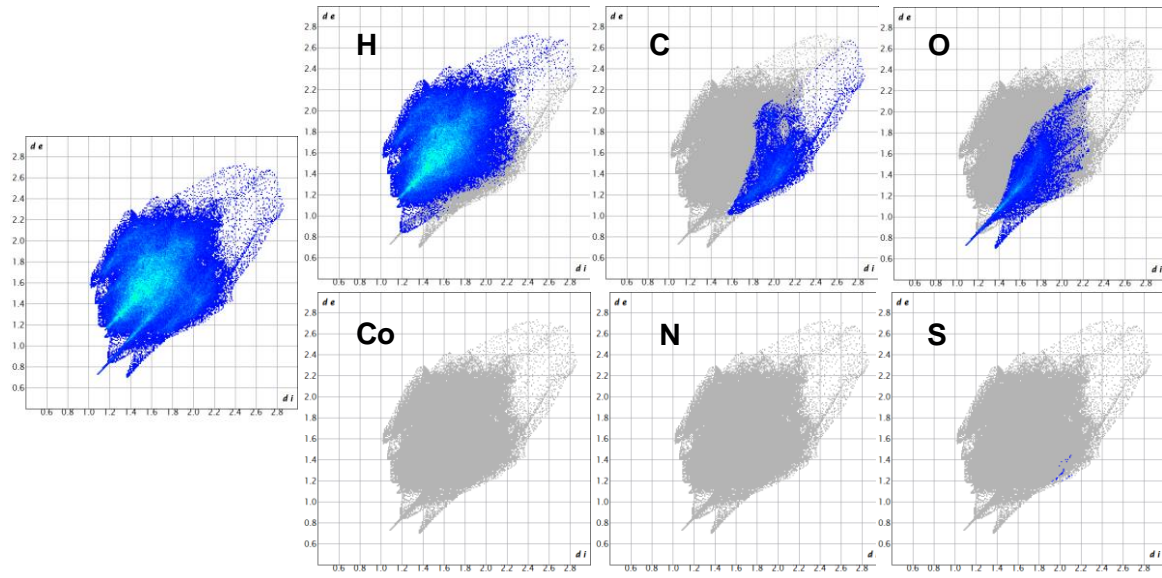


**Figure S12.** Fingerprint plots for the **Co-MST-H<sub>2</sub>O<sup>-</sup>** anion showing the interactions of the listed element inside the Hirshfeld surface to all outer atoms.

### S3. Ni-MST-H<sub>2</sub>O. Additional results

#### S3.a. Powder X-ray diffraction of the Ni-MST-H<sub>2</sub>O sample

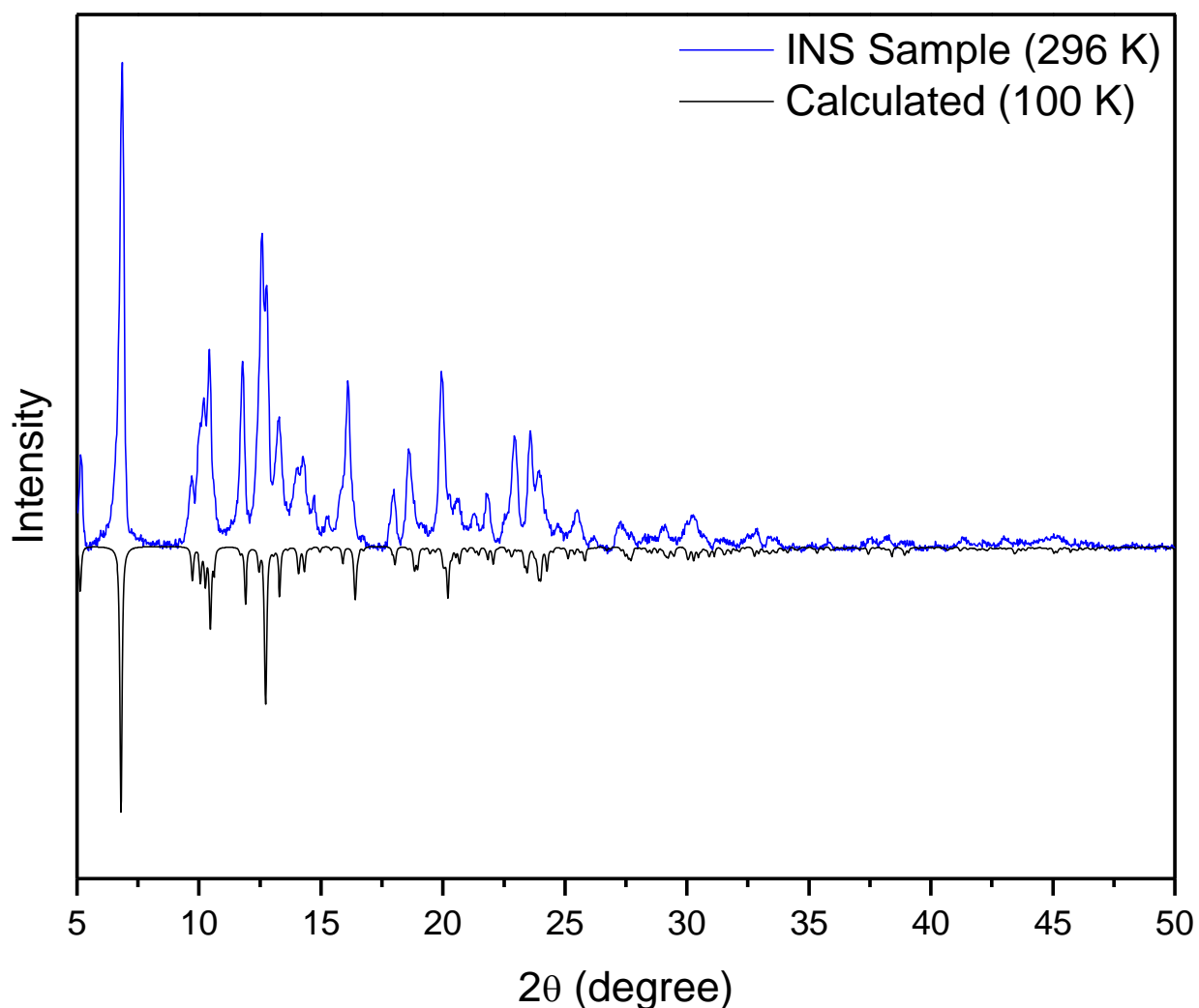


**Figure S13.** PXRD pattern of the Ni-MST-H<sub>2</sub>O sample for INS compared to the calculated pattern from reported structure.<sup>S1</sup>

**S3.b. FIRMS spectra**

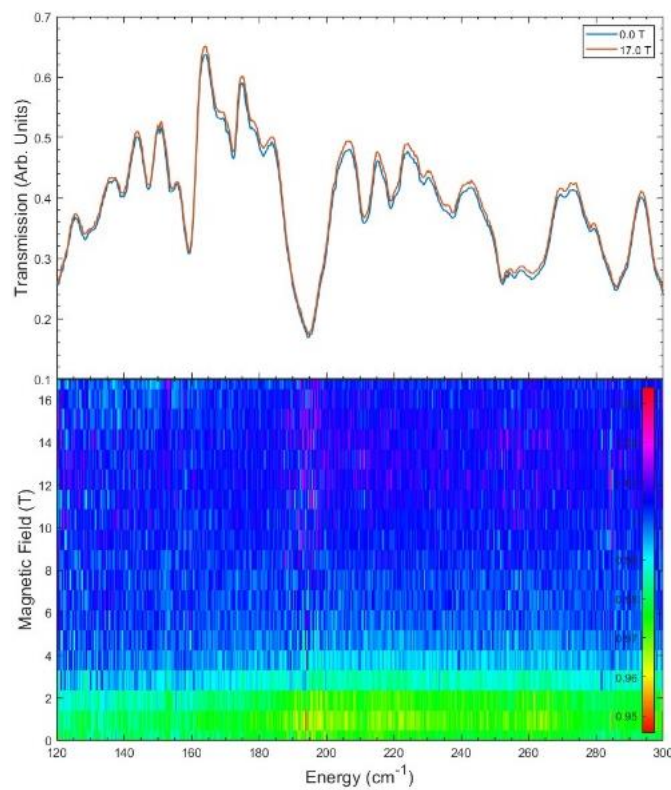


**Figure S14.** FIRMS and contour plot of spectra of **Ni-MST-H<sub>2</sub>O** with no distinct magnetic peak.

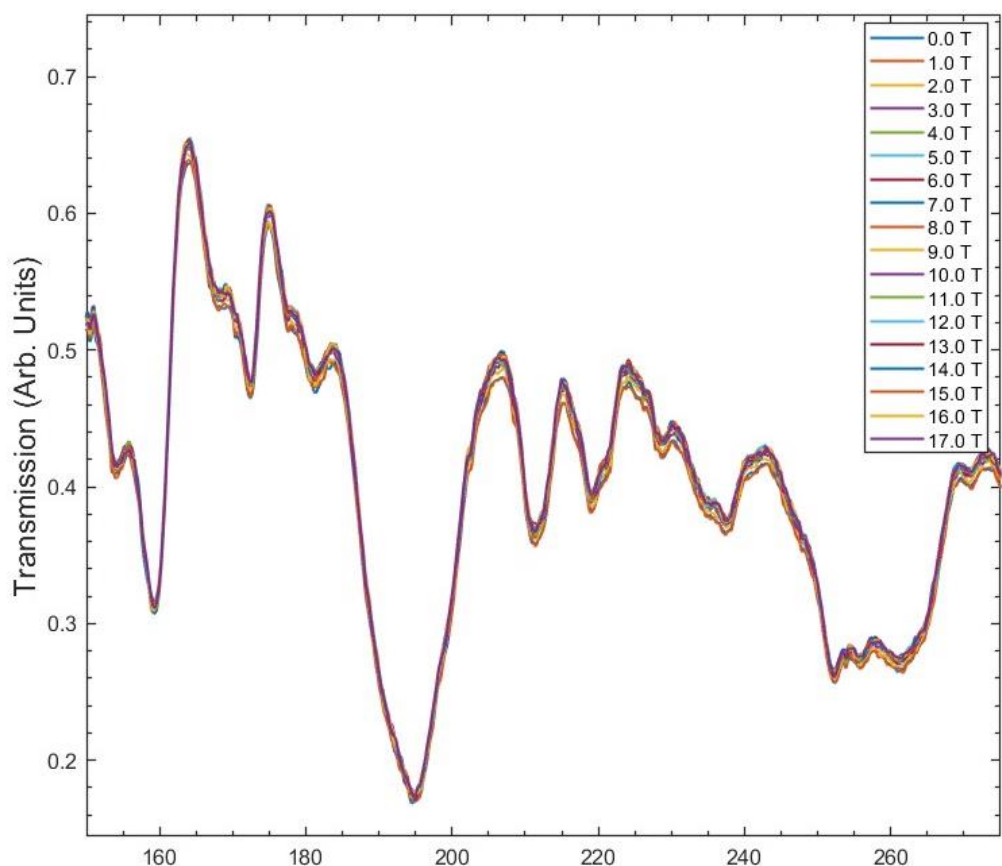


**Figure S15.** Averaged spectral data for **Ni-MST-H<sub>2</sub>O** with all T-values showing vibrational features near the expected magnetic transition. There are several strong phonons in this region, which may couple to magnetic transitions.

**S3.c.** Additional INS spectra

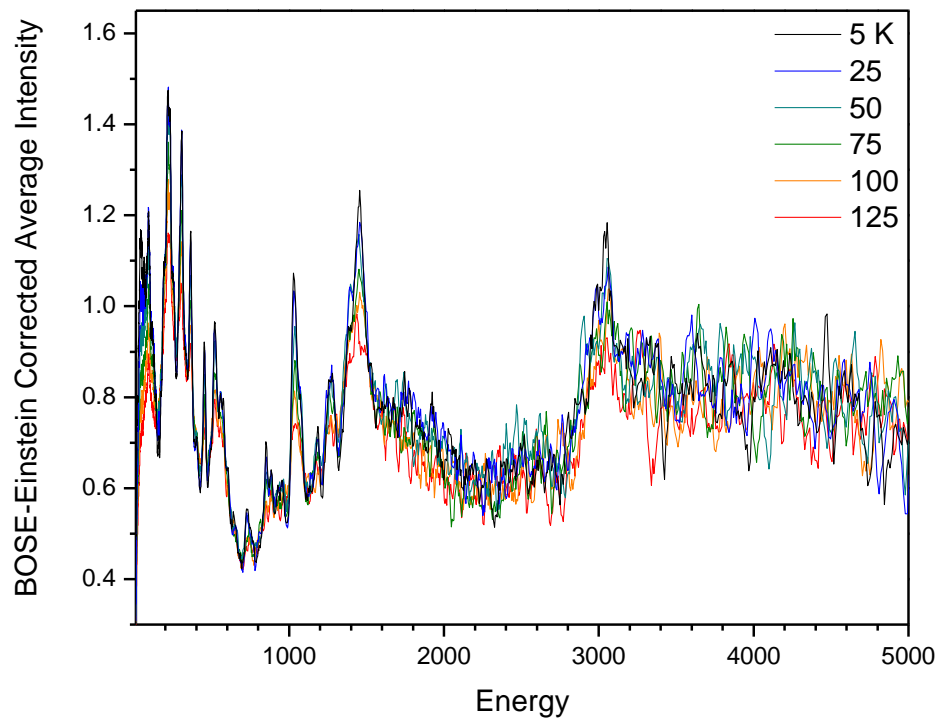


**Figure S16.** INS spectra of **Ni-MST-H<sub>2</sub>O** at 10-5000 cm<sup>-1</sup>.

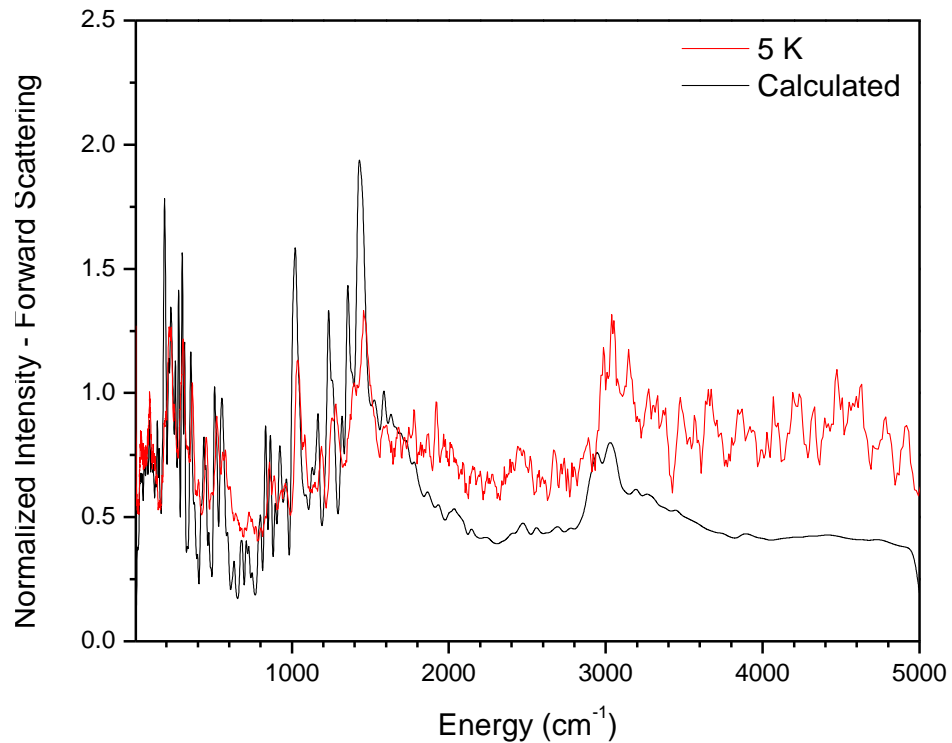


**Figure S17.** Calculated vs experimental spectra of **Ni-MST-H<sub>2</sub>O** at 10-5000 cm<sup>-1</sup>.

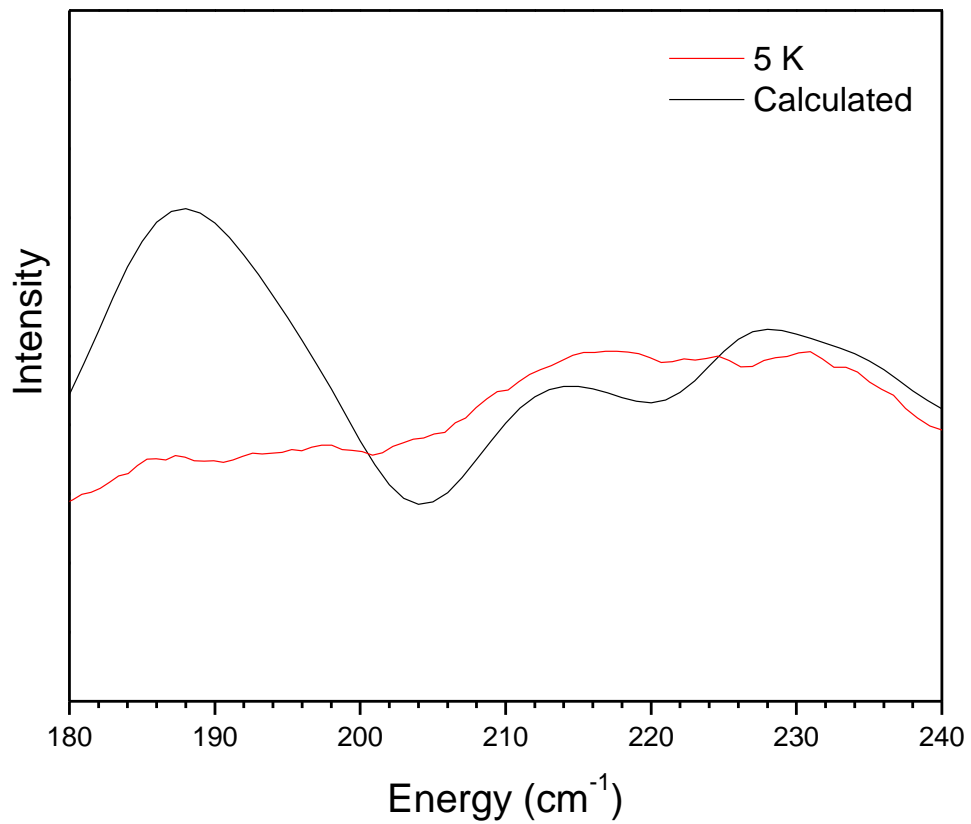


**Figure S18.** INS spectra of **Ni-MST-H<sub>2</sub>O** showing calculated and experimental phonons in the 180-240  $\text{cm}^{-1}$  region.

A comparison of the calculated INS spectrum with observed INS spectrum in the 180-240  $\text{cm}^{-1}$  region in the figure below does not clearly show the magnetic peak.

**S3.c. Hirshfeld surface fingerprint plots**

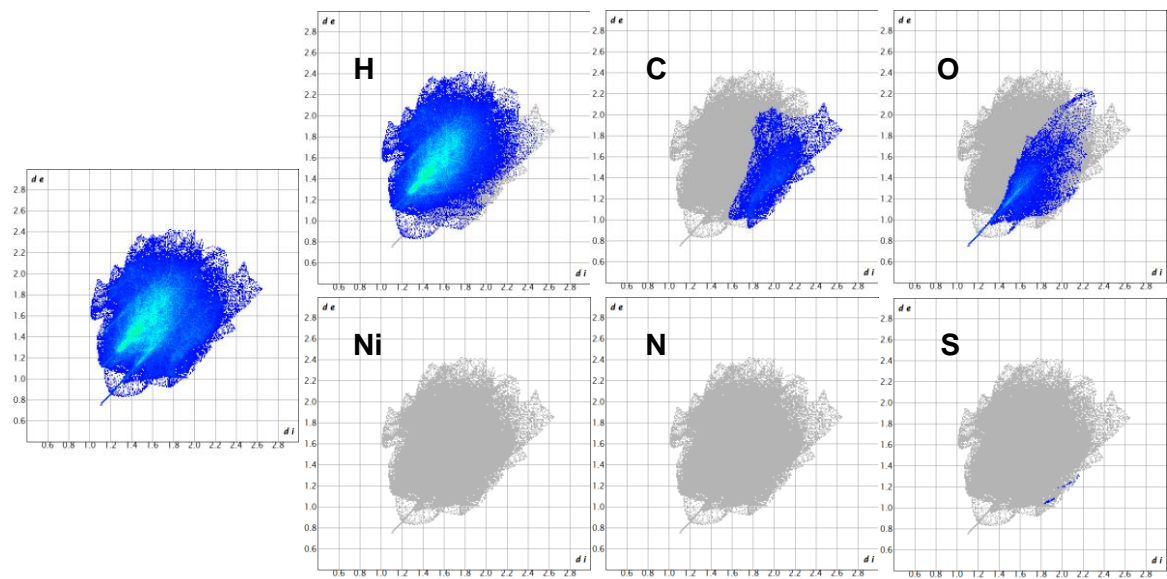


**Figure S19.** Fingerprint plots for **Ni-MST-H<sub>2</sub>O<sup>-</sup>** showing the interactions of the listed element inside the Hirshfeld surface to all outer atoms.

### S3. Spin densities in $[\text{Co}(\text{12-crown-4})_2](\text{I}_3)_2$ and $\text{Co}(\text{AsPh}_3)_2\text{I}_2$

a. Spin densities in  $[\text{Co}(\text{12-crown-4})_2](\text{I}_3)_2$

Single-molecule magnet (SMM) properties of  $[\text{Co}(12\text{-crown-4})_2](\text{I}_3)_2$  were reported by Chen and coworkers.<sup>S4</sup> Its magnetic transitions, spin Hamiltonian parameters, and spin-phonon properties have been probed by advanced spectroscopies.<sup>S5</sup> Its spin densities have been calculated by a DFT calculation similar to that used to calculate the spin densities in **Co-MST-H<sub>2</sub>O**. The spin densities are reported here.

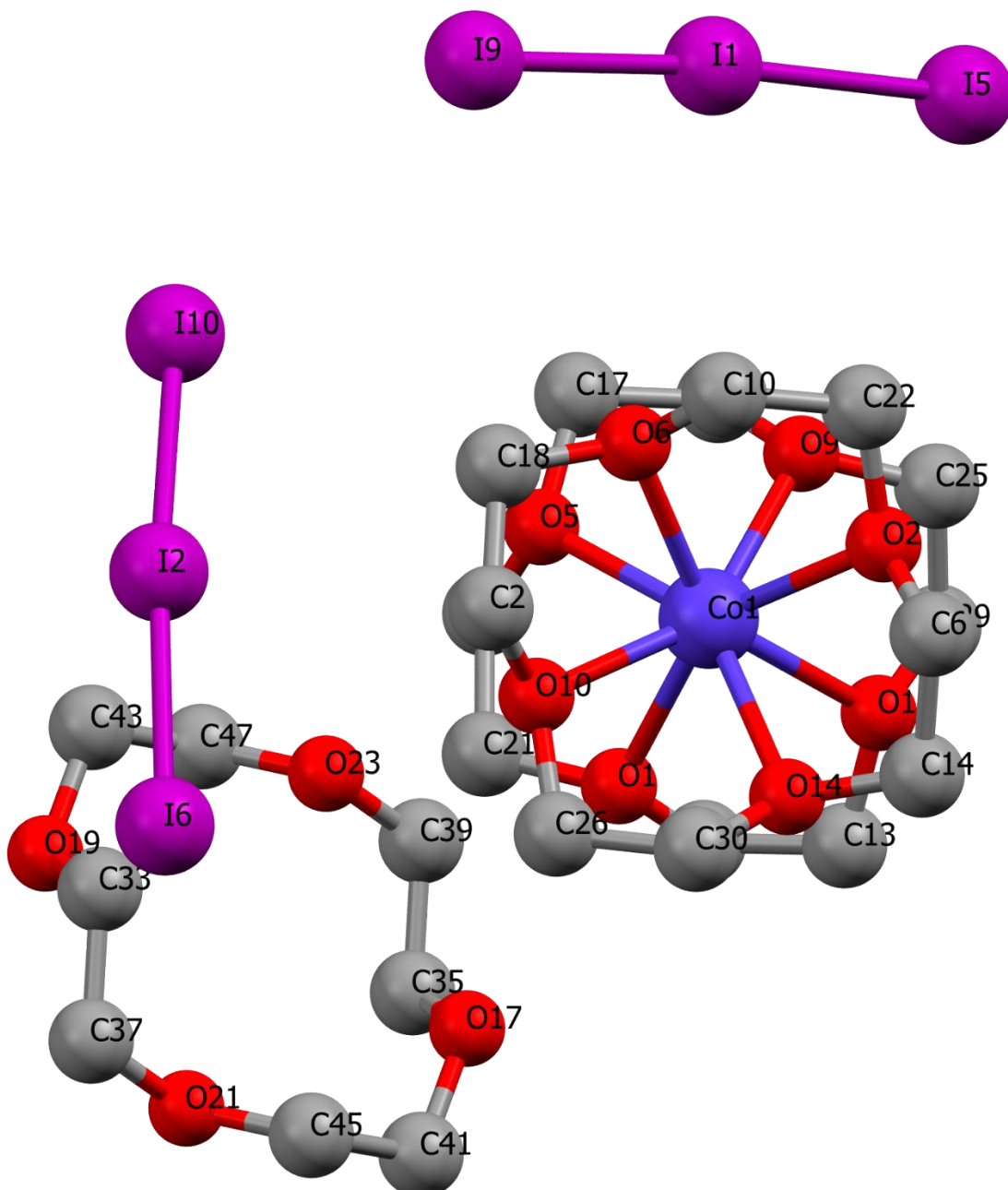


**Table S3.** Spin densities of atoms from VASP calculations for [Co(12-crown-4)<sub>2</sub>](I<sub>3</sub>)<sub>2</sub>. There is a second identical molecule in the lattice and its spin density is not listed.

Atom Label	Spin Density	Atom Label	Spin Density
H1	0.000	H80	0.000
H2	0.000	H82	0.000
H5	0.001	H84	0.000
H6	0.001	H86	0.000
H9	0.000	H88	0.000
H10	0.000	H90	0.000
H13	0.001	H92	0.000
H14	0.001	H94	0.000
H17	0.000	H96	0.000
H18	0.000	C1	0.001
H21	0.001	C2	0.001
H22	0.001	C5	0.001
H25	0.000	C6	0.001
H26	0.000	C9	0.001
H29	0.000	C10	0.001
H30	0.000	C13	0.000
H33	0.000	C14	0.000
H34	0.000	C17	0.000
H37	0.000	C18	0.000
H38	0.000	C21	0.000
H41	0.000	C22	0.000
H42	0.000	C25	0.000
H45	0.000	C26	0.000
H46	0.000	C29	0.001
H49	0.000	C30	0.001
H50	0.000	C33	0.000
H53	0.000	C35	0.000
H54	0.000	C37	0.000
H57	0.000	C39	0.000

H58	0.000	C41	0.000
H61	0.001	C43	0.000
H62	0.001	C45	0.000
H65	0.000	C47	0.000
H66	0.000	O1	0.016
H68	0.000	O2	0.016
H69	0.000	O5	0.017
H72	0.000	O6	0.017
H74	0.000	O9	0.016
H76	0.000	O10	0.016
H78	0.000	O13	0.016
O14	0.016	I1	0.000
O17	0.000	I2	0.000
O19	0.000	I5	0.000
O21	0.000	I6	0.000
O23	0.000	I9	0.000
Co1	2.819	I10	0.000
Total	2.615		

**Table S4.** Summary of spin densities for [Co(12-crown-4)<sub>2</sub>](I<sub>3</sub>)<sub>2</sub>

Atoms	Ranges of spin densities
Co <sup>II</sup>	2.819
O	0.000–0.017
I	0.000
C	0.000–0.001
H	0.000–0.001

b. Spin densities in  $\text{Co}(\text{AsPh}_3)_2\text{I}_2$

Magnetic properties of  $\text{Co}(\text{AsPh}_3)_2\text{I}_2$  were previously studied by Saber and Dunbar, showing slow magnetic relaxation and SMM behavior with easy-axis ZFS ( $D = -74.7 \text{ cm}^{-1}$ ,  $E = -0.82 \text{ cm}^{-1}$ ) from magnetometric studies.<sup>S6</sup> Its spin Hamiltonian parameters and spin-phonon properties have been probed by advanced spectroscopies.<sup>S7</sup> Its spin densities have been calculated by a DFT calculation similar to that used to calculate the spin densities in **Co-MST-H<sub>2</sub>O**. The spin densities are reported here.

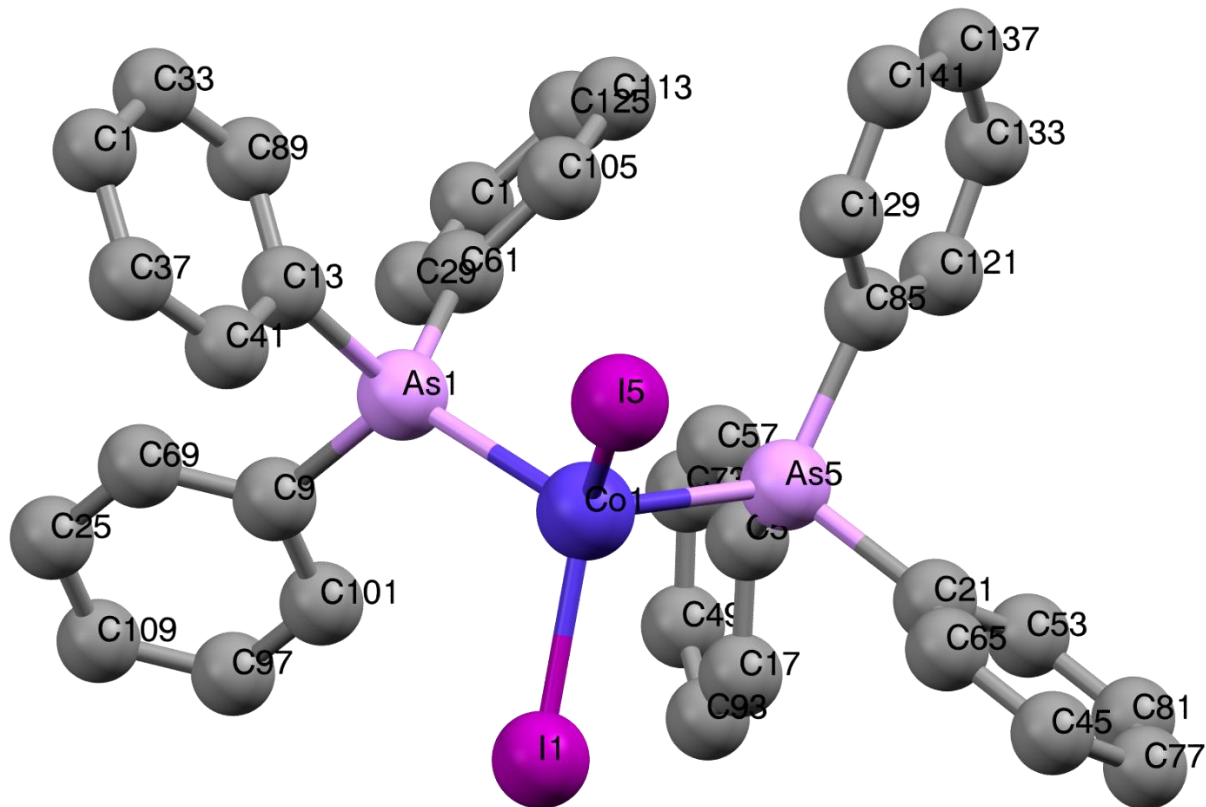


**Table S5.** Spin densities of atoms from VASP calculations for  $\text{Co}(\text{AsPh}_3)_2\text{I}_2$ . There are three other identical molecules in the lattice and their spin densities are not listed.

Atom label	Spin density	Atom label	Spin density
H1	0.000	C25	0.000
H5	0.000	C29	0.001
H9	0.000	C33	0.000

H13	0.000	C37	0.000
H17	0.000	C41	0.000
H21	0.000	C45	0.000
H25	0.000	C49	0.003
H29	0.000	C53	0.001
H33	0.000	C57	0.002
H37	0.000	C61	0.003
H41	0.000	C65	0.000
H45	0.000	C69	0.001
H49	0.000	C73	0.000
H53	0.000	C77	0.000
H57	0.000	C81	0.000
H61	0.000	C85	0.005
H65	0.000	C89	0.001
H69	0.000	C93	0.000
H73	0.000	C97	0.000
H77	0.000	C101	0.000
H81	0.000	C105	0.001
H85	0.000	C109	0.001
H89	0.000	C113	0.000
H93	0.000	C117	0.000
H97	0.000	C121	0.002
H101	0.000	C125	0.001
H105	0.000	C129	0.000
H109	0.000	C133	0.001
H113	0.000	C137	0.000
H117	0.000	C141	0.000
C1	0.001	Co1	2.558
C5	0.003	As1	0.015
C9	0.004	As5	0.019
C13	0.003	I1	0.067
C17	0.003	I5	0.064
C21	0.002	Total	2.7635

**Table S6.** Summary of spin densities for  $\text{Co}(\text{AsPh}_3)_2\text{I}_2$

Atoms	Ranges of spin densities
Co <sup>II</sup>	2.558
I	0.064–0.067
As	0.015–0.019
C	0.000–0.005
H	0.000

## References in SI

- S1. K. A. Schulte, K. R. Vignesh and K. R. Dunbar, Effects of coordination sphere on unusually large zero field splitting and slow magnetic relaxation in trigonally symmetric molecules. *Chem. Sci.*, 2018, **9**, 9018-9026. <https://doi.org/10.1039/C8SC02820F>.
- S2. V. A. S. V. Bittencourt, I. Liberal and S. Viola Kusminskiy, Light propagation and magnon-photon coupling in optically dispersive magnetic media. *Phys. Rev. B*, 2022, **105**, 014409. <https://doi.org/103/PhysRevB.105.014409>.
- S3. Z.-L. Xue, A. J. Ramirez-Cuesta, C. M. Brown, S. Calder, H. Cao, B. C. Chakoumakos, L. L. Daemen, A. Huq, A. I. Kolesnikov, E. Mamontov, A. A. Podlesnyak and X. Wang, Neutron Instruments for Research in Coordination Chemistry. *Eur. J. Inorg. Chem.*, 2019, DOI: 10.1002/ejic.201801076, 1065-1089. <https://doi.org/10.1002/ejic.201801076>.
- S4. L. Chen, J. Wang, J.-M. Wei, W. Wernsdorfer, X.-T. Chen, Y.-Q. Zhang, Y. Song and Z.-L. Xue, Slow Magnetic Relaxation in a Mononuclear Eight-Coordinate Cobalt(II) Complex. *J. Am. Chem. Soc.*, 2014, **136**, 12213-12216. <https://doi.org/10.1021/ja5051605>.
- S5. S. E. Stavretis, D. H. Moseley, F. Fei, H. H. Cui, Y. Cheng, A. A. Podlesnyak, X. Wang, L. L. Daemen, C. M. Hoffmann and M. Ozerov, Spectroscopic Studies of the Magnetic Excitation and Spin-Phonon Couplings in a Single-Molecule Magnet. *Chem. Eur. J.*, 2019, **25**, 15846-15857. <https://doi.org/10.1002/chem.201903635>.
- S6. M. R. Saber and K. R. Dunbar, Ligands effects on the magnetic anisotropy of tetrahedral cobalt complexes. *Chem. Commun.*, 2014, **50**, 12266-12269. <http://doi.org/10.1039/C4CC05724D>.
- S7. D. H. Moseley, Z. Liu, A. N. Bone, S. E. Stavretis, S. K. Singh, M. Atanasov, Z. Lu, M. Ozerov, K. Thirunavukkuarasu, Y. Cheng, L. L. Daemen, D. Lubert-Perquel, D. Smirnov, F. Neese, A. J. Ramirez-Cuesta, S. Hill, K. R. Dunbar and Z.-L. Xue, Comprehensive Studies of Magnetic Transitions and Spin–Phonon Couplings in the Tetrahedral Cobalt Complex Co(AsPh<sub>3</sub>)<sub>2</sub>I<sub>2</sub>. *Inorg. Chem.*, 2022, **61**, 17123-17136. <https://doi.org/10.1021/acs.inorgchem.2c02604>.